

# Basic Principles of Fiber Composite Materials

## 2.1 Introduction to Fiber Composite Systems

A fiber composite material consists of a filamentary phase embedded in a continuous matrix phase. The aspect ratio (i.e., ratio of length to diameter) of the filaments may vary from about 10 to infinity (for continuous fibers). Their scale, in relation to the bulk material, may range from microscopic (e.g., 8- $\mu\text{m}$  diameter carbon fibers in an epoxy matrix) to gross macroscopic (e.g., 25-mm diameter steel bars in concrete).

Composite constituents (fibers and matrices) can be conveniently classified according to their elastic moduli  $E$  and ductility. Within the composite, the fibers may, in general, be in the form of continuous fibers, discontinuous fibers, or whiskers (very fine single crystals with lengths of the order 100–1000  $\mu\text{m}$  and diameters of the order 1–10  $\mu\text{m}$ ) and may be aligned to varying degrees or randomly orientated. This classification is depicted in Figure 2.1 for a number of common fibers and matrices; also listed are examples of composites formed from these materials.

## 2.2 Micromechanical Versus Macromechanical View of Composites

Fiber composites can be studied from two points of view: micromechanics and macromechanics. Micromechanical analyses are aimed at providing an understanding of the behavior of composites, usually those with unidirectional fiber reinforcement, in terms of the properties of the fibers and matrices. Models of varying degrees of sophistication are used to simulate the microstructure of the composite and hence predict its properties (such as strength and stiffness) in terms of the properties and behavior of the constituents.

Macromechanics is the approach used to predict<sup>1</sup> the strength and stiffness of composite structures, as well as other properties such as distortion, on the basis of the “average” properties of the unidirectional material; namely, the longitudinal modulus  $E_1$ , transverse modulus  $E_2$ , major Poisson’s ratio  $\nu_{21}$  and the in-plane shear modulus  $G_{12}$ , as well as the appropriate strength values. A full analysis also

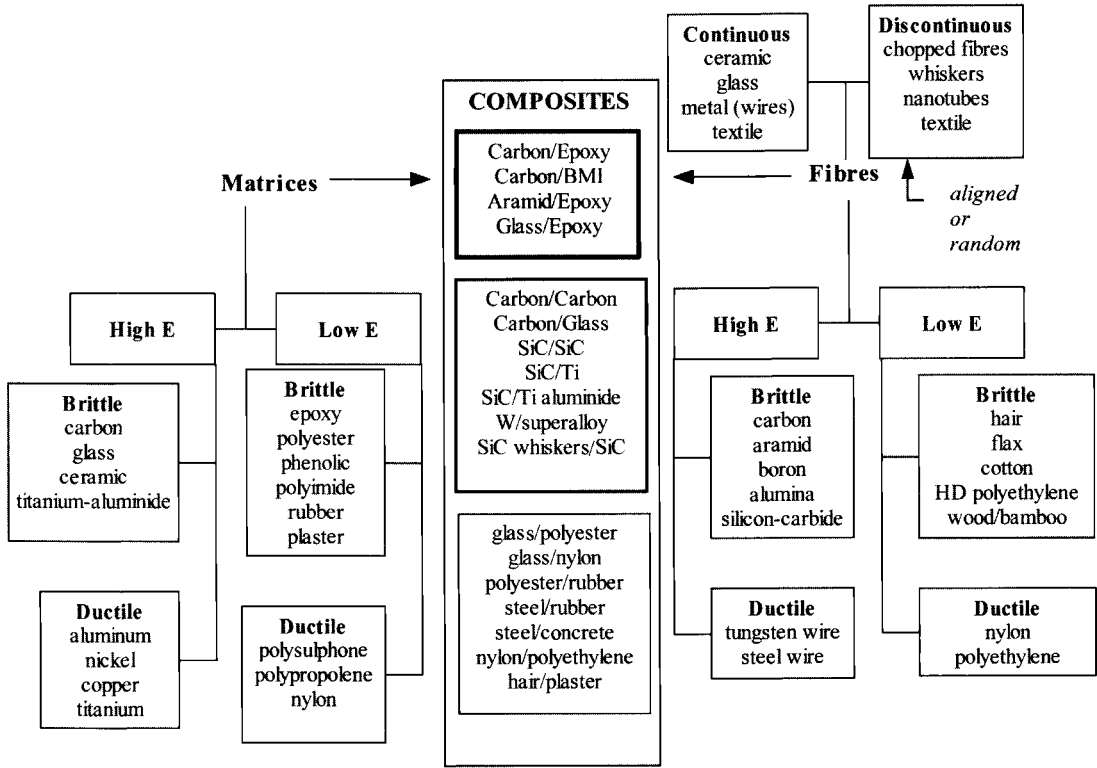


Fig. 2.1 Classification of composites according to fiber and matrix properties.

requires data on the thermal expansion coefficients of the plies in the longitudinal and transverse directions,  $\alpha_1$  and  $\alpha_2$ , respectively.

Composite structural components used in aircraft are most often based on plies (sheets of unidirectional fibers or bi-directionally aligned woven fibers in a matrix) laminated together with the fibers at various orientations, as outlined in Chapter 1. Thus the properties required in the analysis are for a single ply of the composite, as described in Chapter 6. Although this analysis draws largely on data for the plies obtained from physical and mechanical testing of unidirectional composites, estimates of these properties provided by the micromechanical approach can provide useful approximate values of these properties when test data are unavailable.

## 2.3 Micromechanics

As already mentioned, micromechanics utilizes microscopic models of composites, in which the fibers and the matrix are separately modelled. In most simple models, the fibers are assumed to be homogeneous, linearly elastic, isotropic, regularly spaced, perfectly aligned, and of uniform length. The matrix is assumed to be homogeneous, linearly elastic, and isotropic. The fiber/matrix interface is assumed to be perfect, with no voids or disbonds.

More complex models, representing more realistic situations, may include voids, disbonds, flawed fibers (including statistical variations in flaw severity), wavy fibers, non-uniform fiber dispersions, fiber length variations, and residual stresses.

Micromechanics<sup>2</sup> can, itself, be approached in three ways:

- (1) The *mechanics of materials* approach, which attempts to predict the behavior of simplified models of the composite material.
- (2) The *theory of elasticity* approach, which is often aimed at producing upper and lower bound exact analytical or numerical solutions.
- (3) The *finite-element* (F-E) approach based on two-dimensional or three-dimensional models of varying degrees of sophistication.

The most difficult aspect of the composite to model is the fiber/matrix interface, also known as the interphase, which can have a profound effect on strength and toughness. In view of this and other complexities, the F-E micromechanics approach offers by far the best prospect of success to predict strength behavior. Indeed, failure theories, described in Chapter 6, require local modelling at the micromechanical level for predicting the strength of actual components.

A common aim of both approaches is to determine the elastic constants and strengths of composites in terms of their constituent properties. As previously stated, the main elastic constants for unidirectional fiber composites are:

$E_1$  = longitudinal modulus (i.e., modulus in fiber direction)

$E_2$  = transverse modulus

- $\nu_{12}$  = major Poisson's ratio (i.e., ratio of contraction in the transverse direction consequent on an extension in the fiber direction)  
 $G_{12}$  = in-plane shear modulus  
 $\alpha_1$  = longitudinal thermal expansion coefficient  
 $\alpha_2$  = transverse expansion coefficient

The main strength values required are:

- $\sigma_1^u$  = longitudinal strength (both tensile and compressive)  
 $\sigma_2^u$  = transverse strength (both tensile and compressive)  
 $\tau_{12}^u$  = shear strength

where the superscript  $u$  refers to ultimate strength.

## 2.4 Elastic Constants

### 2.4.1 Mechanics of Materials Approach

The simple model used in the following analyses is a single, unidirectional ply, or *lamina*, as depicted in Figure 2.2. Note that the representative volume element shown, is the full thickness of the single ply and that the simplified "two-dimensional" element is used in the following analyses. The key assumptions used in connection with this model are indicated in Figure 2.3.

**2.4.1.1  $E_1$  Longitudinal Modulus.** The representative volume element under an applied stress is shown in Figure 2.3a. The resultant strain  $E$  is assumed to be common to both the fiber and matrix. The stresses felt by the fiber, matrix, and composite are, respectively,  $\sigma_f$ ,  $\sigma_m$ , and  $\sigma_1$ . Taking  $E_f$  and  $E_m$  as the fiber and matrix moduli, respectively, then:

$$\sigma_f = E_f \varepsilon_1, \quad \sigma_m = E_m \varepsilon_1, \quad \sigma_1 = E_1 \varepsilon_1 \quad (2.1)$$

The applied stress acts over a cross-sectional area  $A$  consisting of  $A_f$ , the fiber cross-section, and  $A_m$ , the matrix cross-section. Because the fibers and matrix are acting in parallel to carry the load:

$$\sigma_1 A = \sigma_f A_f + \sigma_m A_m \quad \text{or} \quad \sigma_1 = \sigma_f V_f + \sigma_m V_m \quad (2.2)$$

where  $V_f = A_f/A$  = fiber volume fraction and  $V_m = A_m/A = 1 - V_f$  = matrix volume fraction.

Substituting equation (2.1) into equation (2.2) gives:

$$E_1 = E_f V_f + E_m V_m \quad (2.3)$$

Equation (2.3) is a "rule-of-mixtures" type of relationship that relates the composite property to the weighted sum of the constituent properties.

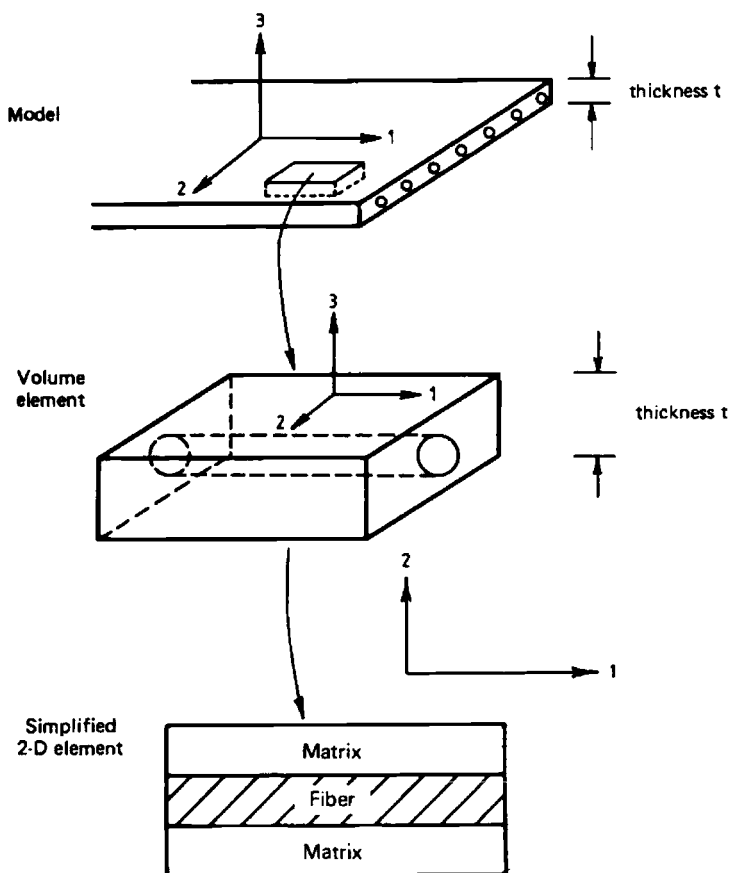


Fig. 2.2 Model and representative volume element of a unidirectional ply.

Experimental verification of equation (2.3) has been obtained for many fiber/resin systems; examples of the variation of  $E_1$  with  $V_f$  for two glass/polyester resin systems are shown in Figure 2.4.

**2.4.1.2  $E_2$  Transverse Modulus.** As shown in Figure 2.3b, the fiber and matrix are assumed to act in series, both carrying the same applied stress  $\sigma_2$ . The transverse strains for the fiber, matrix, and composite are thus, respectively:

$$\varepsilon_f = \frac{\sigma_2}{E'_f}, \quad \varepsilon_m = \frac{\sigma_2}{E_m}, \quad \varepsilon_2 = \frac{\sigma_2}{E_2} \quad (2.4)$$

where  $E'_f$  is the effective transverse modulus of the fiber.

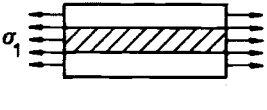
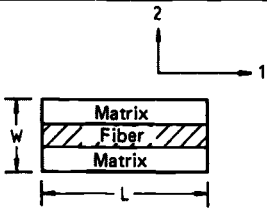
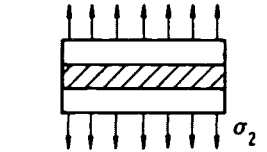
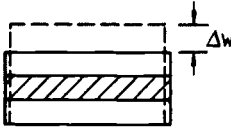
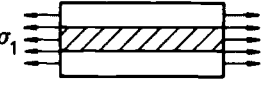
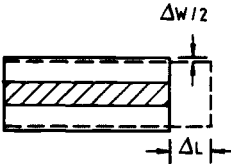
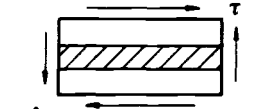
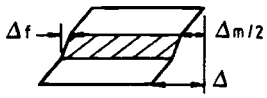
Applied stresses	Deformations	Relationship
<p>a. Determination of <math>E_1</math></p> 	<p>Undeformed element</p> 	$E_1 = E_f V_f + E_m (1 - V_f)$
<p>b. Determination of <math>E_2</math></p> 		$1/E_2 = V_f/E_f + (1 - V_f)/E_m$
<p>c. Determination of <math>\nu_{12}</math></p> 		$\nu_{12} = \nu_f V_f + \nu_m (1 - V_f)$
<p>d. Determination of <math>G_{12}</math></p> 		$1/G_{12} = V_f/G_f + (1 - V_f)/G_m$

Fig. 2.3 Models for the determination of elastic constants by the “mechanics of materials” approach.

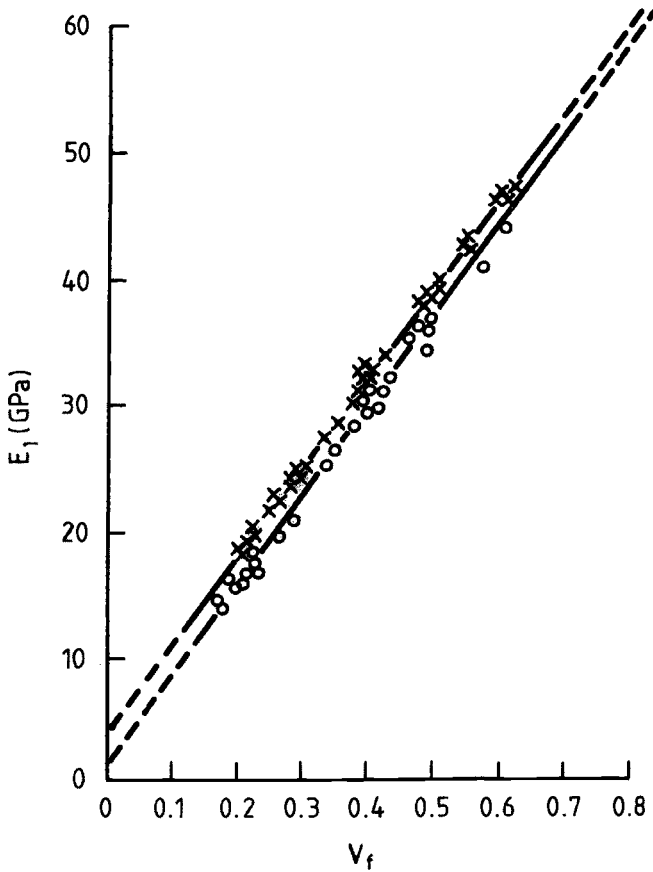


Fig. 2.4  $E_1$  versus fiber volume fraction  $V_f$  for two glass/polyester systems.

Deformations are additive over the width  $W$ , so that:

$$\Delta W = \Delta W_f + \Delta W_m$$

or

$$\varepsilon_2 W = \varepsilon_f (V_f W) + \varepsilon_m (V_m W) \quad (2.5)$$

Substitution of equation (2.4) into equation (2.5) yields:

$$\frac{1}{E_2} = \frac{V_f}{E_f} + \frac{V_m}{E_m} \quad (2.6)$$

Experimental results are in reasonable agreement with equation (2.6) as shown, for example, in Figure 2.5, for a glass/polyester composite.

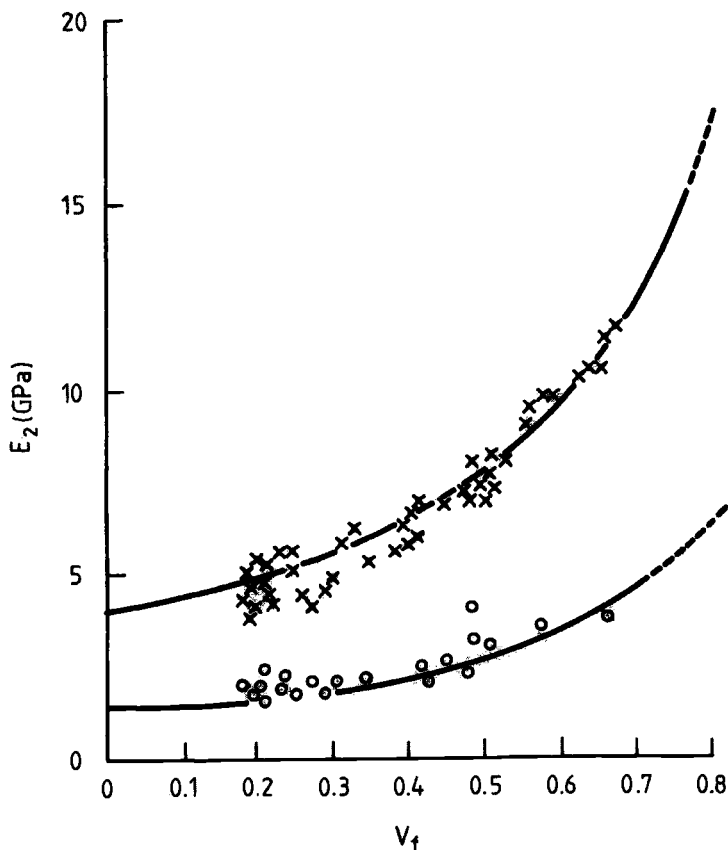


**Fig. 2.5**  $E_2$  versus  $V_f$  for two glass/polyester systems, solid lines are based on Eq. 2.6.

In contrast to glass fibers, which are isotropic, with an  $E_f$  around 72 GPa, carbon fibers are highly anisotropic (stiffness varies with direction), having  $E_f$  around 200 GPa and  $E'_f$  around 7 GPa.

Several interesting features emerge from equations (2.3) and (2.6). In high-performance composites, the fiber moduli are much greater than the resin moduli, so that, in the typical fiber/volume fraction range of 50–60%, the matrix has only a small effect upon  $E_1$  while the fibers have only a small effect on  $E_2$ . In other words,

$$E_1 \approx E_f V_f, \quad E_2 \approx \frac{E_m}{V_m}$$

**2.4.1.3 Major Poisson's Ratio  $\nu_{12}$ .** The major Poisson's ratio is defined by:

$$\nu_{12} = -\frac{\varepsilon_2}{\varepsilon_1} \quad (2.7)$$

where the only applied stress is  $\sigma_1$  (Fig. 2.3c).

The transverse deformation is given by

$$\Delta W = \Delta W_f + \Delta W_m$$

or

$$\varepsilon_2 W = -\nu_f \varepsilon_1 (V_f W) - \nu_m \varepsilon_1 (V_m W) \quad (2.8)$$

Substituting for  $\varepsilon_2$  from equation (2.7) into equation (2.8) gives the result

$$\nu_{12} = \nu_f V_f + \nu_m V_m \quad (2.9)$$

which is another rule-of-mixtures expression.

**2.4.1.4  $G_{12}$  In-Plane Shear Modulus.** The applied shear stresses and resultant deformations of the representative volume element are shown in Figure 2.3d. The shear stresses felt by the fiber and matrix are assumed to be equal, and the composite is assumed to behave linearly in shear (which is, in fact, not true for many systems).

The total shear deformation is given by:

$$\Delta = \gamma W$$

where  $\gamma$  is the shear strain of the composite. The deformation  $\Delta$  consists of two additive components, so that:

$$\gamma W = \gamma_f (V_f W) + \gamma_m (V_m W) \quad (2.10)$$

Because equal shear stresses are assumed:

$$\gamma_f = \frac{\tau}{G_f}, \quad \gamma_m = \frac{\tau}{G_m}, \quad \gamma = \tau/G_{12} \quad (2.11)$$

substitution of equation (2.11) into equation (2.10) yields:

$$\frac{1}{G_{12}} = \frac{V_f}{G_f} + \frac{V_m}{G_m} \quad (2.12)$$

Because  $G_m$  is much smaller than  $G_f$ , the value of  $G_m$  has the major effect on  $G_{12}$  for typical 50–60%  $V_f$  values; the situation is analogous to that for the transverse modulus  $E_2$ .

## 2.4.2 Refinements to Mechanics of Materials Approach for $E_1$ and $E_2$

**2.4.2.1 Prediction of  $E_1$ .** Equation (2.3) is considered to provide a good estimate of the longitudinal modulus  $E_1$ ; however it does not allow for the triaxial stress condition in the matrix resulting from the constraint caused by the fibers. Ekvall<sup>3</sup> has produced a modified version of the equation to allow for this effect

$$E_1 = E_f V_f + E'_m V_m \quad (2.13)$$

where

$$E'_m = \frac{E_m}{(1 - 2\nu_m^2)}$$

and  $\nu_m$  is Poisson's ratio for the matrix material. However, the modification is not large for values of  $\nu_m$  of approximately 0.3.

**2.4.2.2 Prediction of  $E_2$ .** Equation (2.6) is considered to provide only an approximate estimate of the transverse modulus  $E_2$ . This is because, for loading in the transverse direction, biaxial effects resulting from differences in contraction in the longitudinal (fiber) direction between the fiber and the matrix become significant. The contraction difference arises because the two phases experience different strains, and this is even more marked if there is a difference in their Poisson's ratios.

The modified version of equation (2.6) produced by Ekvall<sup>3</sup> is

$$\frac{1}{E_2} = \frac{V_f}{E_f} + \frac{V_m}{E_m} - \frac{V_f [(E_f \nu_m / E_m) - \nu_f]^2}{E_f [(V_f E_f / V_m E_m) + 1]} \quad (2.14)$$

## 2.4.3 Theory of Elasticity Approach to the Elastic Constants

The theory of elasticity approach to the determination of the elastic constants for composites is based on a wide variety of models and energy balance treatments. A detailed discussion of these approaches is beyond the scope of this chapter; however, some aspects are outlined here.

**2.4.3.1 Energy Approach.** Bounding (or variational) derivations use energy balance considerations to produce upper and lower bounds on the elastic constants. The usefulness of the results, of course, depends upon the closeness of the bounds, as demonstrated in the following example.

Considering the stressed element shown in Figure 2.3a, it can be shown<sup>4</sup> that the lower bound on the longitudinal modulus  $E_1$  is given by:

$$\frac{1}{E_1} \leq \frac{V_m}{E_m} + \frac{V_f}{E_f} \quad (2.15)$$

Compare with equation (2.6), while the upper bound is given by:

$$E_1 \leq \frac{1 - \nu_f - 4\nu_f\nu_{12} + 2\nu_{12}^2}{1 - \nu_f - 2\nu_f^2} E_f V_f + \frac{1 - \nu_m - 4\nu_m\nu_{12} + 2\nu_{12}^2}{1 - \nu_m - 2\nu_m^2} E_m V_m \quad (2.16)$$

where

$$\nu_{12} = \frac{(1 - \nu_m - 2\nu_m^2)\nu_f E_f V_f + (1 - \nu_f - 2\nu_f^2)\nu_m E_m V_m}{(1 - \nu_m - 2\nu_m^2)E_f V_f + (1 - \nu_f - 2\nu_f^2)E_m V_m}$$

It is of interest to note that if  $\nu_{12} = \nu_f = \nu_m$ , the upper bound solution becomes:

$$E_1 \leq E_f V_f + E_m V_m$$

which is the same result as equation (2.3), which implies an equality of  $\nu_f$  and  $\nu_m$  in the mechanics of materials approach.

In this example, the bounding solutions are not very useful because the bounds are too far apart, the lower bound being the transverse modulus as predicted by the mechanics of materials approach.

**2.4.3.2 Direct Approaches.** Here, various representative models of elastic inclusions in an elastic matrix are employed to obtain exact solutions for the stiffness properties. Typical volume elements assumed for a hexagonal and a square fiber distribution are shown in Figure 2.6. In many cases, the solutions are highly complex and of limited practical use. Regular fiber distributions do not occur in practical composites. Rather, the array is random and the analysis for regular arrays must be modified to allow for the extent of contact between fibers. This is called the *degree of contiguity*<sup>5</sup> and is measured by a coefficient  $c$ , which can vary from  $c = 0$  for isolated fibers to  $c = 1$  for contacting fibers. This situation is illustrated in Figure 2.7. The effective value of  $c$  may be determined experimentally. The degree of contiguity has more effect on  $E_2$  and  $G_{12}$  than on  $E_1$ . These matters, and other simplifying approaches, such as the Halpin-Tsai equations, are discussed more fully in Ref. 5.

## 2.4.4 Expansion Constants $\alpha_1$ and $\alpha_2$

The coefficients of thermal expansion  $\alpha_1$  and  $\alpha_2$  for the unidirectional ply are required, for example, in the thermomechanical analysis of multidirectional laminates.

The actual values of the two constants derive from the expansion coefficients of the fibers  $\alpha_f$  and matrix  $\alpha_m$ , and their orientation. Differences between  $\alpha_f$  and

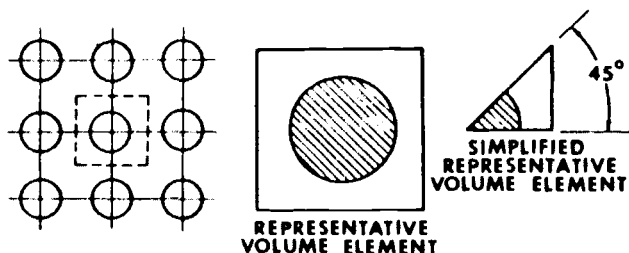
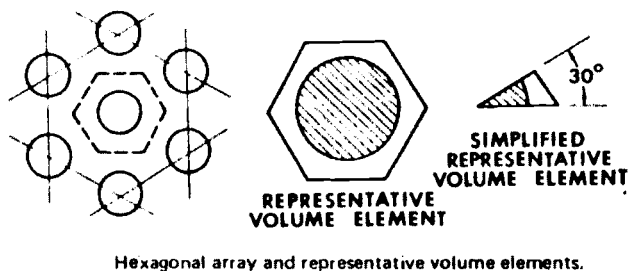


Fig. 2.6 Typical models of composites for exact elasticity solutions.

$\alpha_m$  give rise to internal stresses and possibly distortion when cooling laminates after manufacture and during subsequent service.

2.4.4.1 *Longitudinal Expansion Coefficient  $\alpha_1$ .* A simple estimate of  $\alpha_1$  can be made based on the model in Figure 2.3 used to estimate  $E_1$ . We have that:

$$\epsilon_1 = \epsilon_f = \epsilon_m = \frac{\sigma_f}{E_f} + \alpha_f \Delta T = \frac{\sigma_m}{E_m} + \alpha_m \Delta T$$

where  $\Delta T$  = temperature change.

Also, since there are no external stresses:

$$\sigma_f V_f = -\sigma_m(1 - V_f)$$

This leads to:

$$\alpha_1 = \frac{E_f \alpha_f V_f + E_m \alpha_m (1 - V_f)}{E_f V_f + E_m (1 - V_f)} \tag{2.17}$$

Because, in many composites,  $\alpha_f \ll \alpha_m$  the  $\alpha_f$  term can be ignored in the equation.

2.4.4.2 *Transverse Expansion Coefficient  $\alpha_2$ .* A simple rule-of-mixtures estimate of  $\alpha_2$  is obtained assuming the series model used in Figure 2.3. To

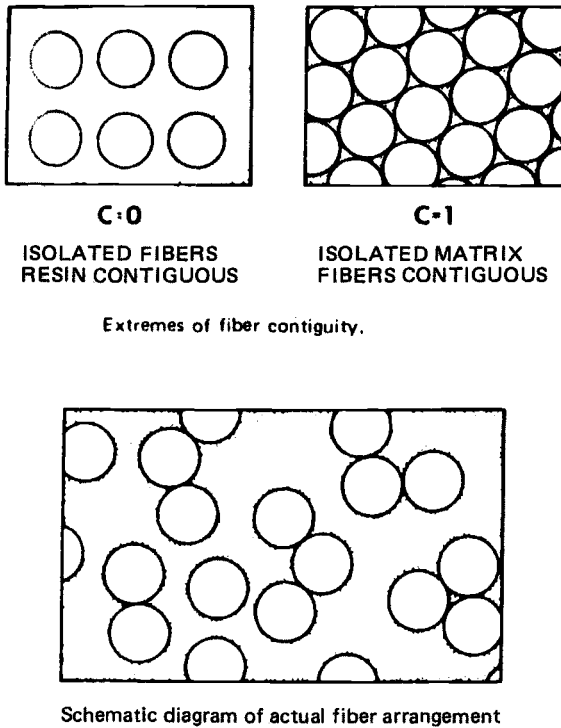


Fig. 2.7 Concept of contiguity used for semi-empirical-elasticity solutions.

estimate  $E_2$  we have that

$$\alpha_2 = \alpha'_f V_f + \alpha_m (1 - V_f) \quad (2.18)$$

where  $\alpha'_f$  is the transverse expansion coefficient for the fiber, which often differs significantly from the longitudinal value  $\alpha_f$ . Carbon fibers represent an extreme case of variation because the fiber is highly anisotropic. Thus, although  $\alpha_f$  is around 0, the  $\alpha'_f$  is around  $10^{-6} \text{C}^{-1}$ . For the epoxy resin  $\alpha_m = 55 \times 10^{-6} \text{C}^{-1}$

However, this model does not account for any interaction between the fiber and matrix, due in part to ignoring differences in Poisson's ratio, and leads to the conclusion that there are no thermally induced stresses between the fiber and matrix.

If interaction is included, it can be shown<sup>2</sup> that:

$$\alpha_2 = \alpha'_f V_f + \alpha_m (1 - V_f) + \left( \frac{E'_f \nu_m - E_m \nu_m}{E_1} \right) (\alpha_m - \alpha_f) (1 - V_f) V_f \quad (2.19)$$

## 2.5 Micromechanics Approach to Strength

### 2.5.1 Simple Estimate of Tensile Strength

The simplest analysis of longitudinal tensile strength assumes that all fibers break at the same stress level, at the same time, and in the same plane. Although this assumption is grossly unrealistic, it provides a useful starting point for more realistic analysis.

As with the model used to determine  $E_1$ , the fibers and matrix are assumed to experience equal strains. In advanced epoxy/matrix composites, the strain-to-failure capability of the stiff fibers  $\epsilon_f^u$  is markedly less than that of the matrix  $\epsilon_m^u$ , as shown in Figure 2.8a. The fibers will thus fail first, and the total load will be transferred to the matrix. Two composite failure modes can be envisaged depending on the fiber volume fraction  $V_f$ . At high  $V_f$ , the matrix alone is not capable of bearing the full load and fractures immediately after fiber fracture. The composite strength is thus given by

$$\sigma_1^u = \sigma_f^u V_f + \sigma_m' V_m \quad (2.20)$$

where  $\sigma_f^u$  is the fiber failure stress and  $\sigma_m'$  is defined in Figure 2.8a as the stress carried by the matrix material at the fiber breaking strain. At low  $V_f$ , there is enough matrix material to carry the full load after the fibers fracture; the composite strength is then given by

$$\sigma_1^u = \sigma_m^u V_m$$

$\sigma_1^u$  is plotted as a function of  $V_f$  in Figure 2.8b, where it can be readily seen that the value of  $V_f$  corresponding to a change in the failure mode is given by:

$$V_f' = \frac{(\sigma_m^u - \sigma_m')}{(\sigma_f^u + \sigma_m^u - \sigma_m')} \quad (2.21)$$

Note also that there is a minimum volume fraction  $V_{\min}$  below which composite strength is actually less than the inherent matrix strength.

$$V_{\min} = \frac{(\sigma_m^u - \sigma_m')}{(\sigma_f^u - \sigma_m')} \quad (2.22)$$

For high-strength, high-modulus fibers in relatively weak, low-modulus epoxy matrices,  $\sigma_m' V_f$  and  $V_{\min}$  will be quite small.

Analogous treatments can be applied to systems in which the matrix fails first, but obviously the physical characteristics and consequences of the fracture modes will be quite different. With composites having a metal matrix, consideration must be given to yielding of the matrix. Ref. 6, discuss this issue with respect to strength and other relevant mechanical properties.

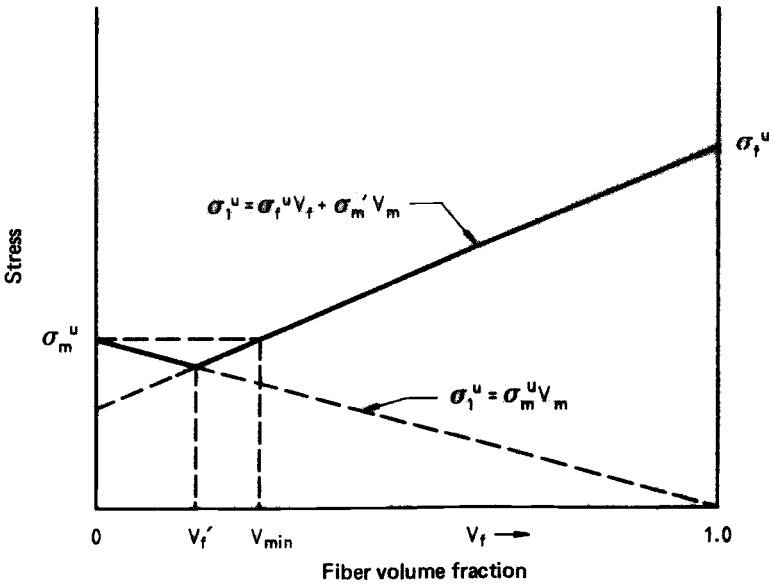
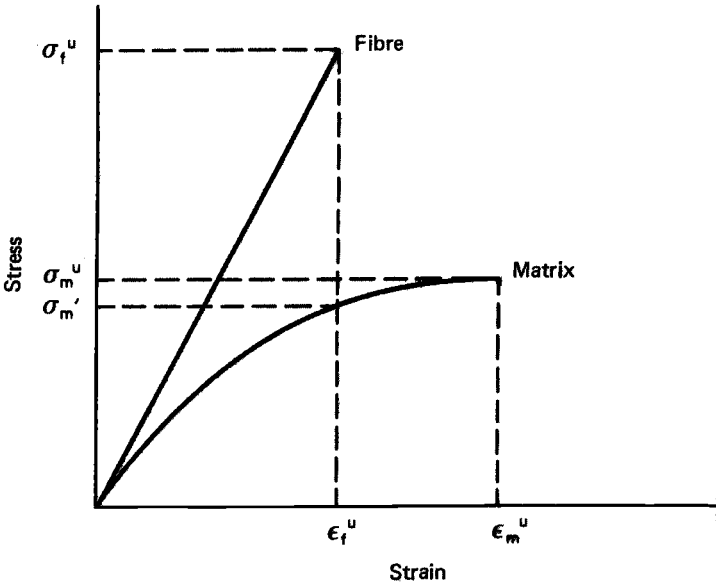


Fig. 2.8 Rule of mixtures prediction of  $\sigma_1^u$  for  $\epsilon_f^u < \epsilon_m^u$ .

### 2.5.2 Statistical Analysis of Tensile Strength

The foregoing analysis of tensile strength assumed simultaneous fracture of equal-strength fibers in one plane. In reality, the situation is much more complex because of the brittle (flaw-sensitive) nature of the fibers and the fiber/matrix interaction. These two features are discussed below.

Brittle fibers contain surface flaws or imperfections that produce “weak spots” along the fiber length. Fiber fractures will occur at these flaws at more or less random positions throughout the composite. Therefore, fracture will not occur in a single plane. In the simplest case, in which the imperfect fibers all have the same strength and the matrix is unable to grip the broken fibers, the strength of the composite would be calculated as in the previous subsection.

For brittle fibers, however, flaws vary not only in position, but also in severity. The way in which the fiber strength changes as a result of this variation in the flaw severity is shown in Figure 2.9 for a typical case. Therefore, it would be expected that fiber fractures would occur throughout a range of stress levels, up to ultimate composite failure. This is indeed the case, as shown in Figure 2.10.

Another important characteristic of composite fracture is the fiber/matrix interaction in the vicinity of a fiber fracture. Rather than becoming ineffective, a broken fiber can still contribute to composite strength because the matrix is able to transfer stress back into the fiber from the broken end, as shown in Figure 2.11. High shear stresses develop in the matrix and then decay a short distance from the break; at the same time, the tensile stress carried by the fiber increases from zero at the broken end to the full stress carried by unbroken fibers. The characteristic length over which this stress build up occurs is known as the ineffective length  $\delta$  (See Fig. 2.11). Often, the term *critical transfer length* is used in this context, the critical transfer length being twice the ineffective length.

The ineffective length  $\delta$  can be determined experimentally by measuring the stress required to pull fibers of various lengths from a matrix.<sup>7</sup>

If the fiber/matrix bond strength is low, the high shear stresses will cause fiber/matrix debonding, as shown in Figure 2.12a. It is also possible that the stress elevation felt by fibers adjacent to the fractured fiber (Figure 2.11) is sufficient to cause further fiber fractures and crack propagation through the matrix in the brittle fashion shown in Figure 2.12b. In addition to the stress concentration felt by fibers resulting from the ineffectiveness of adjacent fractured fibers near the broken ends, there is also a stress concentration associated with the crack in the matrix surrounding the fiber fracture.

If fiber/matrix debonding, crack propagation, and fiber fracture propagation are not the dominant failure mechanisms, the composite will accumulate damage under increasing stress and failure will occur by the cumulative damage mechanism outlined below and shown in Figure 2.12c.

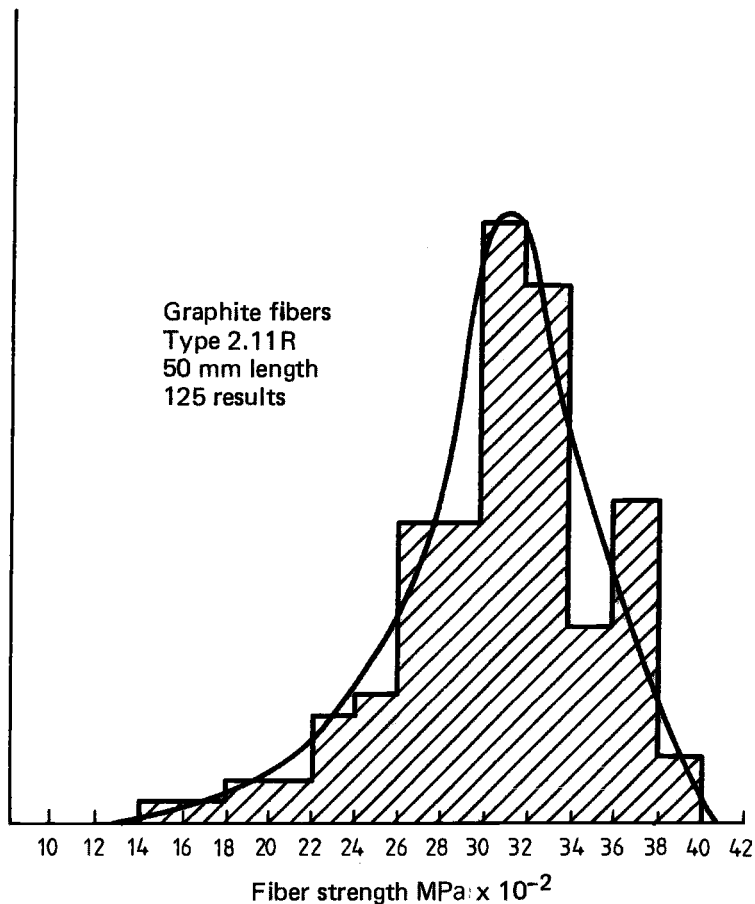


**Fig. 2.9** Plot of number of observations versus strength for carbon fibers, showing typical strength distribution.

### 2.5.3 Rosen's Model of Cumulative Damage

The strength of individual fibers is dependent on the probability of finding a flaw and, therefore, is dependent on the fiber length. It has been shown that the strength/length relationship takes the form of a Weibull distribution of the form:

$$f(\sigma) = L\alpha\beta\sigma^{\beta-1}\exp(-L\alpha\sigma^\beta)$$

where  $f(\sigma)$  is the probability density function for fiber strength  $\sigma$ ,  $L$  is the fiber length, and  $\alpha$  and  $\beta$  are the material constants.

Constant  $\alpha$  determines the position of the Weibull distribution, while constant  $\beta$  determines its shape. Both  $\alpha$  and  $\beta$  are experimentally accessible quantities and

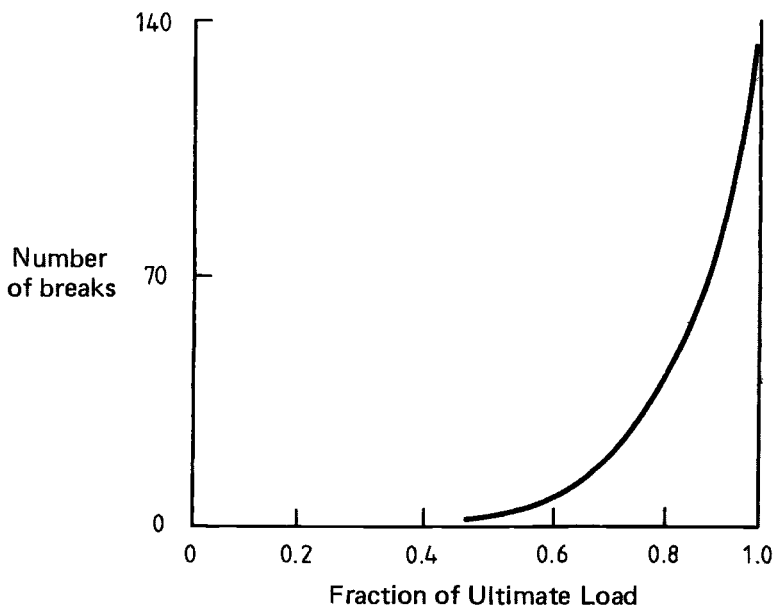


Fig. 2.10 Number of fiber fractures versus fraction of ultimate composite strength.

can be determined, for example, from a log-log plot of mean fiber strength for fibers of given lengths versus fiber length.

Daniels<sup>8</sup> showed that the strength of a bundle of  $N$  fibers having such a Weibull distribution can be described by a normal distribution where the mean value  $\bar{\sigma}_{BL}$  is a function of fiber length:

$$\bar{\sigma}_{BL} = (L\alpha\beta)^{-1/\beta} \exp\left(\frac{-1}{\beta}\right) \quad (2.23)$$

and whose standard deviation is proportional to  $N^{-1/2}$ . Thus, for very large  $N$ , all of the bundles tend toward the same strength value  $\sigma_{BL}$ .

Rosen<sup>9</sup> models the composite as a chain of bundles (Figure 2.13), the length of each bundle (or chain link) being the ineffective length  $\delta$ . For very large  $N$ , the strength of each bundle or chain link will be the same, and the strength of the whole chain (or composite) will be equal to the link strength, which is given by:

$$\bar{\sigma}_{B\delta} = (\delta\alpha\beta)^{-1/\beta} \exp\left(\frac{-1}{\beta}\right) \quad (2.24)$$

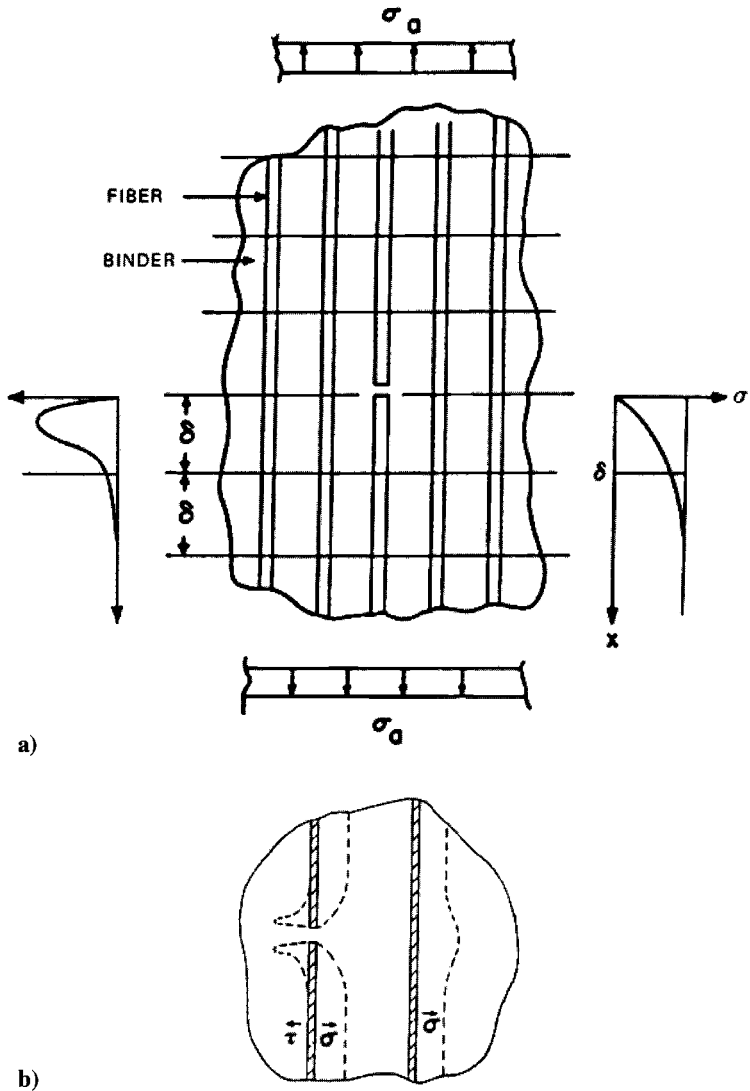
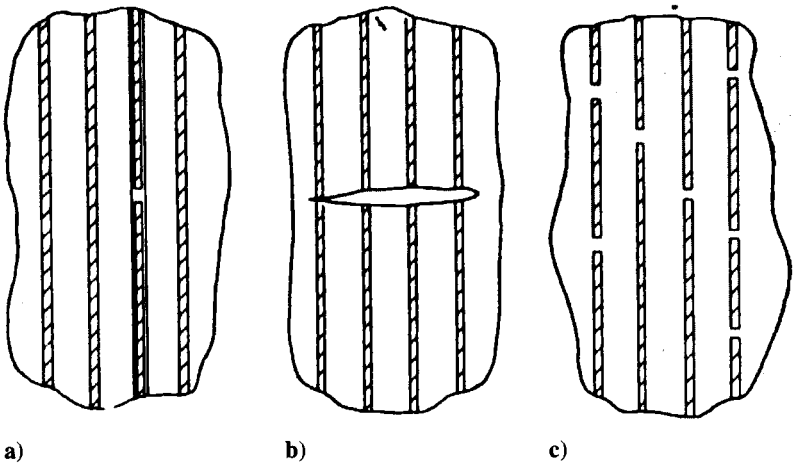


Fig. 2.11 Rosen's model showing a) ineffective length at break and b) perturbation of stress in adjacent fiber.

Thus, it is possible to compare the strengths of a bundle of "dry" fibers of length  $L$  and a composite with ineffective length  $\delta$  as follows:

$$\frac{\bar{\sigma}_{B\delta}}{\bar{\sigma}_{BL}} = \left(\frac{L}{\delta}\right)^{1/\beta} \quad (2.25)$$



**Fig. 2.12 Possible composite tensile failure modes: a) fiber bundle; b) crack; c) statistical.**

For carbon fibers in an epoxy matrix,  $\beta \cong 10$  and  $\delta = 10^{-2}$  mm (about a fiber diameter), so if  $L = 100$  mm, then:

$$\frac{\bar{\sigma}_{B\delta}}{\bar{\sigma}_{BL}} = \left( \frac{100}{10^{-2}} \right)^{1/10} \cong 2.5$$

This is the strengthening obtained by composite action.

## 2.6 Simple Estimate of Compressive Strength

The previously introduced equations relating to tensile failure do not apply to compressive strength because fibers do not fail in simple compression. Rather, they fail by local buckling. The actual behavior is very complicated because, to the external stresses, it is influenced by the presence of residual stresses in the matrix caused by the difference between fiber and matrix expansion coefficients. It has been shown, for example, that glass fibers in an epoxy matrix can buckle simply after cooling down from the resin cure temperature. As may be expected, when it is assumed that the fibers act as circular columns on an elastic foundation, the wavelength of the buckling increases with the fiber diameter.

Two pure buckling modes can be envisaged (See Fig. 2.14): 1) the shear mode in which the fibers buckle in-phase and the matrix is sheared or 2) the extensional mode, in which the matrix is stretched and compressed in an out-of-phase manner. The most likely mode is that producing the lowest energy in the system. While mixed modes are possible, they require more energy than do either of the pure modes.

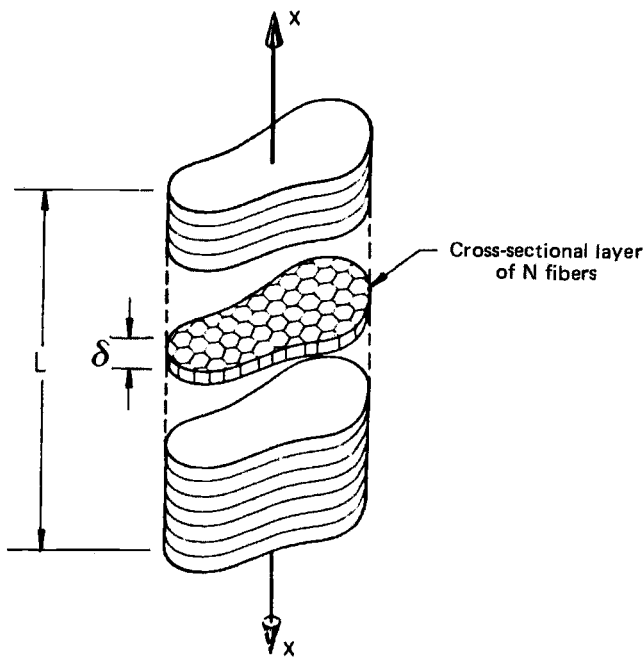


**Fig. 2.13** Rosen's model showing chain of fiber bundles.

Analysis of the buckling<sup>1</sup> is based on the energy method in which the change in strain energy of the fibers  $\Delta U_f$  and of the matrix  $\Delta U_m$  is equated to the work done  $\Delta W$  by the external loads as the composite changes from the compressed but unbuckled state to the buckled state.

$$\Delta U_f + \Delta U_m = \Delta W \quad (2.26)$$

In the model, the composite is considered two-dimensional, the fibers are treated as plates normal to the plane of Figure 2.15 (rather than rods), and the buckling pattern is assumed to be sinusoidal. The resulting buckling stress for the extensional mode is:

$$\sigma_{c \max} \cong 2V_f \left[ \frac{V_f E_m E_f}{3(1 - V_f)} \right]^{1/2} \quad (2.27)$$

and for the shear mode:

$$\sigma_{c \max} = \frac{G_m}{(1 - V_f)} \quad (2.28)$$

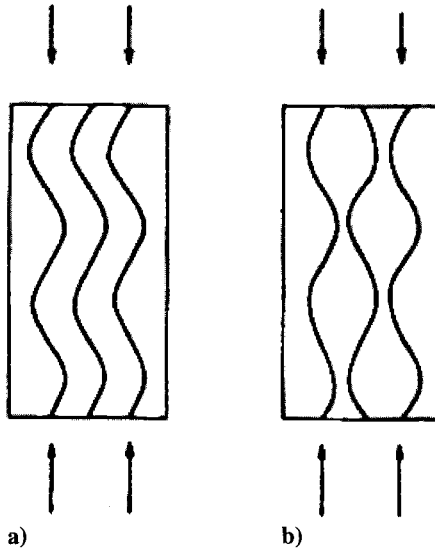


**Fig. 2.14** Two pure buckling modes for unidirectional composites in compression: a) shear or in-phase mode; b) extension or out-of-phase mode.

As  $V_f$  tends to zero,  $\sigma_{c \max}$  for the extensional mode tends to zero; but, as  $V_f$  tends to unity,  $\sigma_{c \max}$  for the extensional mode becomes very large compared with  $\sigma_{c \max}$  for the shear mode. Thus, the extensional mode would be expected to apply for only small  $V_f$ . Assuming  $E_f \gg E_m$  and  $\nu_m = 1/3$ , with  $G_m = E_m/2(1 + \nu_m)$ , then the transition occurs at  $(E_m/10E_f)^{1/3}$ , or at  $V_f = 10\%$  for  $E_f/E_m = 100$ , and at  $V_f = 22\%$  for  $E_f/E_m = 10$ .

It has been found that these equations overpredict the compressive strength considerably. In the case of boron/epoxy, the actual compressive strength is about 63% lower than that predicted, while for other material combinations the prediction can be worse. Generally the problem is that the predicted failure strains are much higher than the matrix yield strain. As an approximation to the inelastic behavior, the theory was expanded (Ref. 10) using a gradually reducing matrix shear modulus. This gives more reasonable agreement with experimental results.

A very simple approach that appears to predict the experimental behavior in some cases is obtained by assuming failure occurs when the matrix reaches its yield stress  $\sigma_m^y$ . Thus, at failure:

$$\sigma_{c \max} = \sigma_f V_f + \sigma_m^y V_m \quad (2.29)$$

where the fiber stress is given by strain compatibility as:

$$\sigma_f = \frac{\sigma_m^y E_f}{E_m} = \epsilon_m^y E_f \quad (2.30)$$

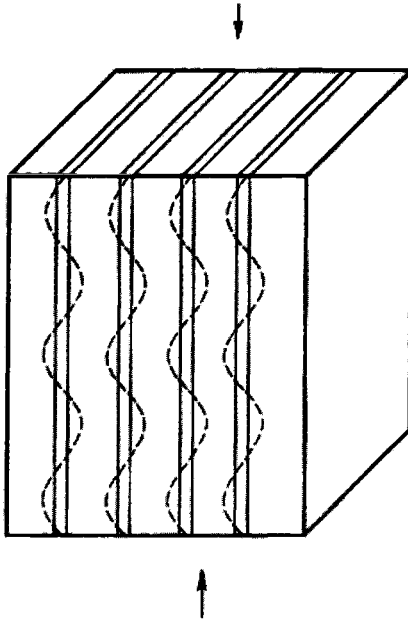


Fig. 2.15 Model for buckling fibers in a unidirectional composite.

taking  $\varepsilon_m^y$  for an epoxy resin as 0.02 and  $E_f = 70$  GPa for glass fibers, then

$$\sigma_f = 0.02 \times 70 \text{ GPa} = 1.4 \text{ GPa}$$

and so:

$$\sigma_c^u = \sigma_f V_f = 1.4 \times 0.6 = 0.84 \text{ GPa}$$

(ignoring the small contribution from the matrix).

This result is in more reasonable agreement with typically observed values.

## 2.7 Off-Axis Strength in Tension

The failure of an orientated, but still unidirectional composite can be envisaged as occurring in any of three modes:

- (1) Failure normal to the fibers (as occurs with straight tension in the fiber direction)
- (2) Failure parallel to the fibers by matrix rupture or fiber/matrix interface tensile failure

(3) Failure by shear of the matrix or fiber/matrix interface If the fibers make an angle  $\phi$  with the direction of applied tensile stress  $\sigma$ , then, as shown in Figure 2.16, the stresses can be resolved as follows:

Tensile stress parallel to fibers  $\sigma_1 = \sigma \cos^2 \phi$

Tensile stress normal to fibers  $\sigma_2 = \sigma \sin^2 \phi$

Shear stress parallel to fibers  $\tau_{12} = \frac{1}{2}\sigma \sin 2\phi$

If  $\sigma_1^u$ ,  $\sigma_2^u$  and  $\tau^u$  represent the composite strengths in direct tension ( $\phi = 0^\circ$ ), transverse tension ( $\phi = 90^\circ$ ), and shear ( $\phi = 45^\circ$ ), respectively, then the failure stress for each mode can be expressed as:

Mode 1:  $\sigma = \frac{\sigma_1^u}{\cos^2 \phi}$

Mode 2:  $\sigma = \frac{\sigma_2^u}{\sin^2 \phi}$  (2.31)

Mode 3:  $\sigma = \frac{2\tau_u}{\sin 2\phi}$

Thus, the failure mode changes with  $\phi$  as shown in Figure 2.17. Although these results are obeyed quite well for many systems and the observed fracture modes

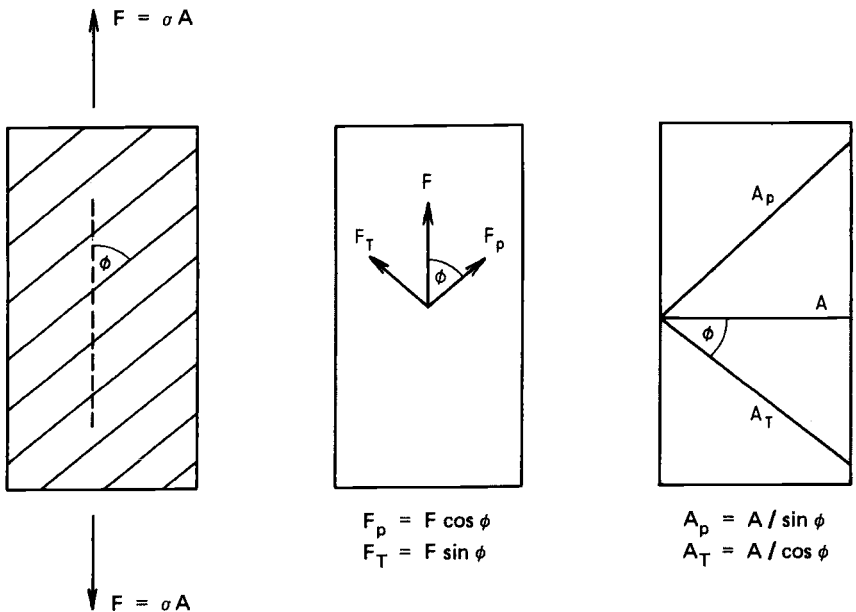
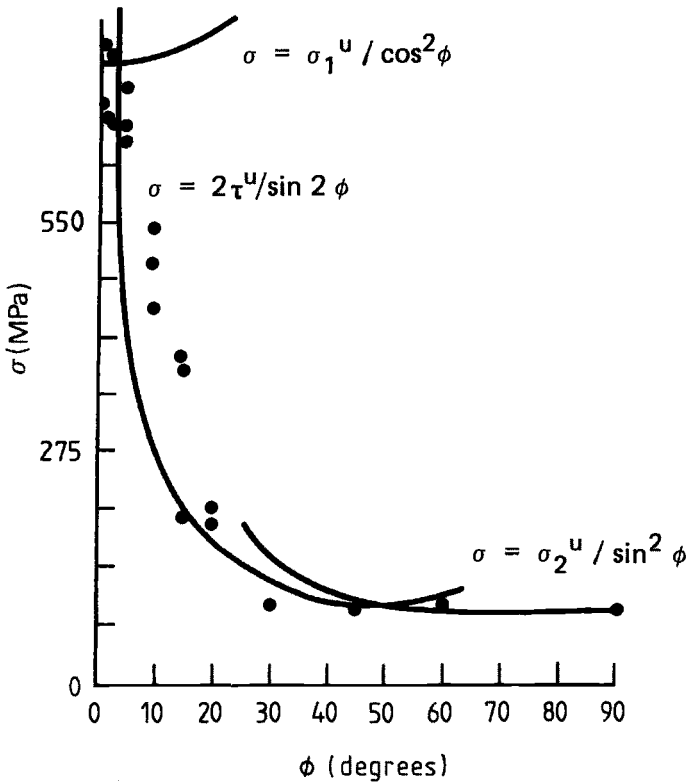


Fig. 2.16 Resolution of forces and areas in off-axis tension.



**Fig. 2.17** Example of the variation of tensile strength versus orientation for a unidirectional composite.

are as predicted, the interaction of stresses and the occurrence of mixed-mode fractures are not accounted for. Ref. 1 presents a more detailed analysis that accounts for the complex stress states.

Figure 2.17 shows that strength falls rapidly with increasing  $\phi$ . However, if the plies are placed at  $+\phi$  and  $-\phi$ , the rate of fall-off is very much less, even to values of  $\phi$  as high as  $30^\circ$ . The reasons for this are intuitively obvious because the plies reinforce each other against mode 1 or mode 2 failure.

## 2.8 Fracture Toughness of Unidirectional Composites

### 2.8.1 Fracture Surface Energy

A measure of the toughness, or the resistance of a material to crack propagation, is its fracture surface energy  $\gamma$ . This is defined as the minimum amount of energy required to create a unit area of free surface (crack) and is

usually given in units of  $\text{kJ m}^{-2}$ . Because two free surfaces are produced,  $R$  (for crack resistance) equal to  $2\gamma$  is the term often employed in fracture calculations.

It is a matter of considerable importance that, for crack propagation normal to the fibers (Fig. 2.18a), the fracture energy of a composite consisting of brittle fibers in a brittle matrix is usually much greater than is predicted by a simple rule-of-mixtures relationship. In general,  $R_1 \gg V_f R_f + V_m R_m$ . For example, in the case of a typical carbon/epoxy composite,  $R_m \approx 1 \text{ kJ m}^{-2}$  for the bulk epoxy resin and  $R_f \approx 0.1 \text{ kJ m}^{-2}$  for the carbon fiber. However, the fracture surface

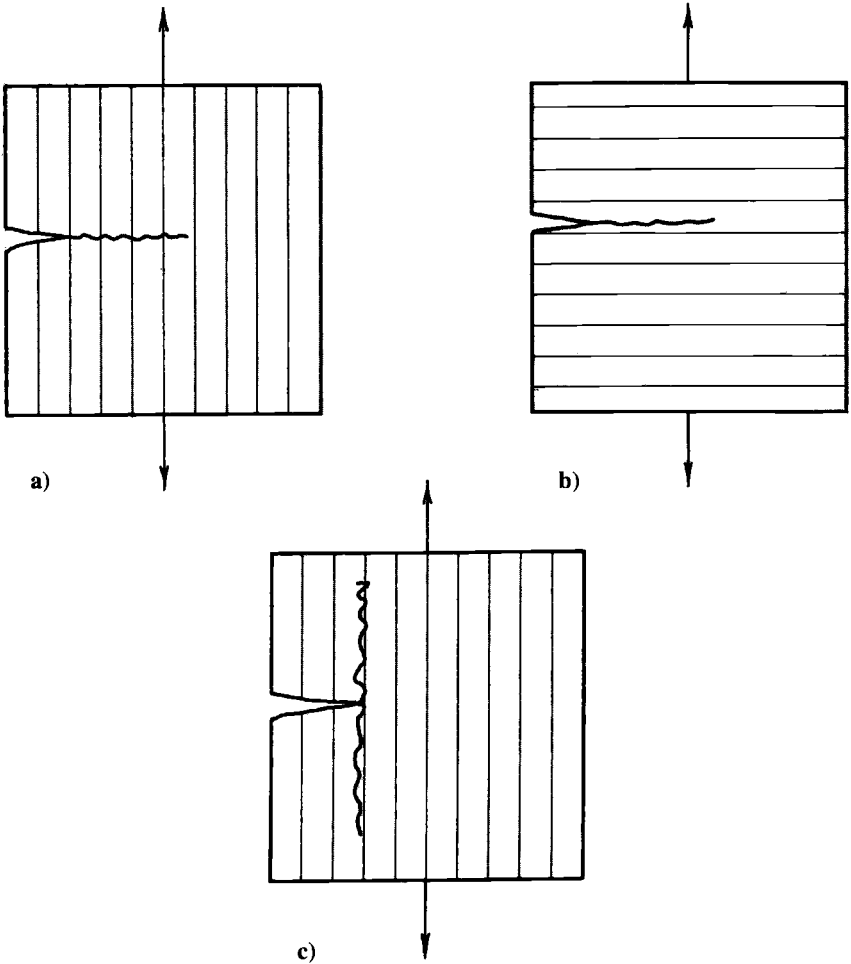


**Fig. 2.18** Three basic modes of crack propagation in unidirectional fiber composites subject to simple tensile loading: *a)* normal to the fibers; *b)* parallel to the fibers; and *c)* crack deflection along the fibers, or splitting. Modes *a* and *b* are self-similar modes of propagation.

energy of a unidirectional composite  $R_c$  (if the crack is forced to propagate normal to the fibers) is typically  $25\text{--}50 \text{ kJ m}^{-2}$ .

In contrast, for crack propagation parallel to the fibers (Fig. 2.18b), the fracture surface energy  $R_2$  is of the order of  $R_m$  if the crack propagates solely through the matrix; however  $R_m$  will be lower if the crack propagates partially through the weaker fiber/matrix interface. Because  $R_2 \ll R_1$ , crack propagation parallel to the fibers, or splitting (Fig. 2.18c), will generally result even when the starting crack is normal to the fibers.

Considering crack propagation normal to the fibers (Fig. 2.18a), the total work of fracture can be attributed to a number of sources<sup>11,12</sup> as shown in Figure 2.19 and Table 2.1 taken from Ref. 11. In the case of the brittle fiber/brittle matrix composite (Fig. 2.19a), crack growth proceeds by pulling fibers out of the matrix behind the crack front and by fracturing fibers ahead of the crack tip. Energy is absorbed during *pull-out* if the shear stress at the fiber/matrix interface is maintained while the fracture surface is separating. If the fiber/matrix interface is relatively weak, local stresses will cause the fibers to be *debonded* from the matrix, with a resultant loss of stored strain energy. Stored strain energy is also lost by *stress relaxation* over the transfer length when the fiber fractures. Finally, strain energy is also lost from the fiber by crack bridging if the fiber spans the opening crack before fracture.

If the matrix is ductile, as in a metal-matrix composite, energy is also absorbed by *matrix plastic deformation*. This situation is illustrated in Figure 2.19b for the case in which the fiber is strongly bonded to the matrix so that little fiber *pull-out* occurs.

The work of the fracture contribution for *pull-out* in Table 2.1 refers to short constant-strength fibers. The expression would have to be modified for a statistical flaw distribution in continuous fibers. The contribution due to creation of new surfaces of fibers and matrix can be ignored in brittle systems, as can contributions from the matrix yield.

### 2.8.2 Fracture Mechanics

The energetic requirement for crack propagation is that the energy-release rate (equal to the “fixed grips” strain energy release rate)  $G$  must equal the fracture surface energy  $R$ . At the critical condition,

$$G = G_c = R \quad (2.32)$$

In many cases, it is more convenient to work in terms of the stress intensity factor  $K$ . For an isotropic material in the crack opening mode,  $K_I$  is related to  $G$  through the equation  $K_I^2 = EG$  and  $K_{Ic}^2 = EG_c$  at failure.

In the simple case of a small centre crack in a sheet under tension:

$$K_I = \sigma(\pi a)^{1/2} \quad (2.33)$$

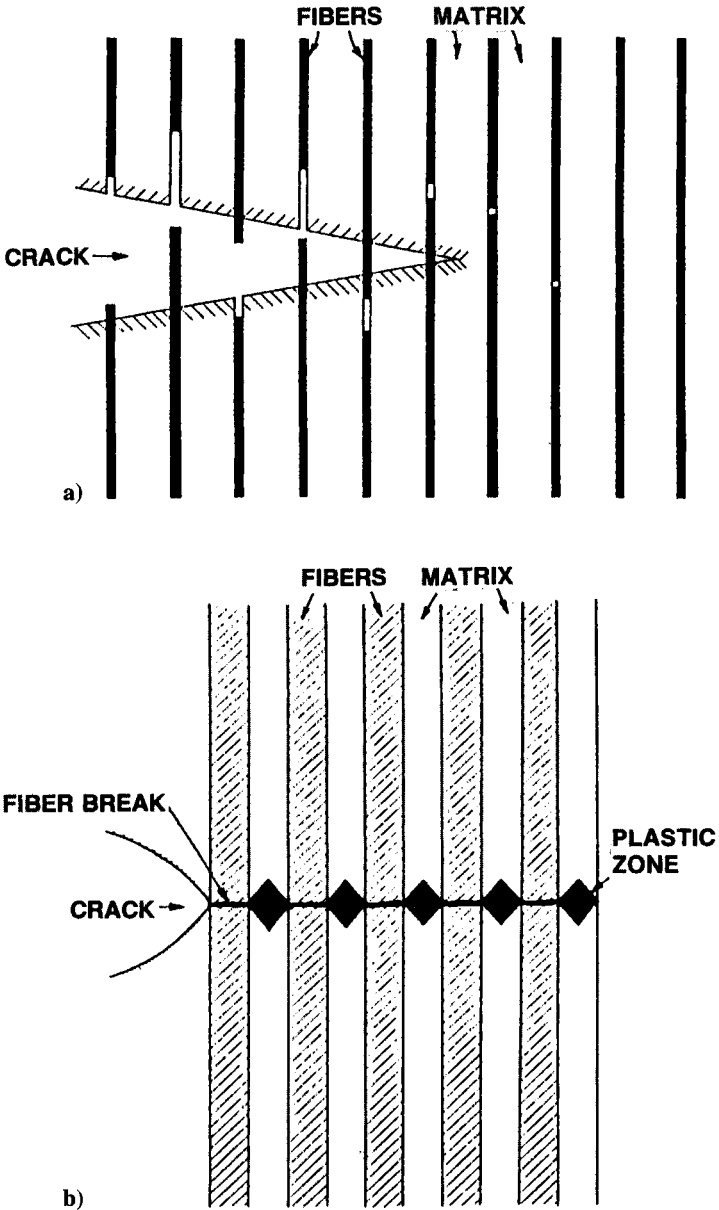


Fig. 2.19 Fracture behavior during failure of *a*) a brittle fiber/brittle matrix composite and *b*) a brittle fiber/ductile matrix composite where the fibers are assumed to be strongly bonded to the matrix.

**Table 2.1 Models for Contributions to Work of Fracture for a Discontinuous Fiber Composite, Taken from Ref. 11**

Model	$\gamma$
Pull-out (short fibers of length $L$ )	$\frac{V_f \sigma_f^\mu \delta^2}{3L} (L > 2\delta)$ $\frac{V_f \sigma_f^\mu L^2}{24\delta} (L < 2\delta)$
Debonding	$\frac{V_f (\sigma_f^\mu)^2 y}{4E_f}$
Stress relaxation	$\leq \frac{V_f (\sigma_f^\mu)^2 \delta}{3E_f}$
Crack bridging	$\frac{2V_f r (\sigma_f^\mu)^3}{\tau_i E_f} \times \frac{(1 - \nu_f)(1 - 2\nu_f)}{12(1 - \nu_f)}$
Matrix plastic deformation	$\frac{(1 - V_f)^2}{V_f} \times \frac{\sigma_m^\mu r}{\tau_m} \times U$

where  $\sigma$  is the applied stress and  $2a$  the crack length. Thus, the stress  $\sigma_F$  at failure is given by

$$\sigma_F = \left( \frac{ER}{\pi a} \right)^{1/2} \tag{2.34}$$

which is the familiar Griffith equation.<sup>13</sup>

A relationship between  $G$  and  $K$  can also be obtained for a fiber composite material by modelling it as a continuous linear orthotropic material with the crack propagating on one of the planes of symmetry. Using the analysis for such materials given in Ref. 14,

$$G = K_I^2 \left( \frac{a_{11} a_{22}}{2} \right)^{1/2} \left[ \left( \frac{a_{22}}{a_{11}} \right)^{1/2} + \left( \frac{a_{66} + 2a_{12}}{2a_{11}} \right) \right]^{1/2} \tag{2.35}$$

Here the  $a_{ij}$  terms are the coefficients of the stresses in the stress-strain law defined using a coordinate system based not on the fiber direction, but on the crack in the “1 direction” and the load in the “2 direction”. This seems to be conventional in fracture mechanics treatments of this type. The factor involving the  $a$  terms can be considered as the reciprocal of the effective modulus  $E'$  of the composite. For the simple case illustrated in Figure 2.18a, where the crack is perpendicular to the fiber direction:

$$a_{22} = \frac{1}{E_{11}}, \quad a_{11} = \frac{1}{E_{22}}, \quad a_{66} = \frac{1}{G_{12}}$$

$$a_{12} = -\frac{\nu_{12}}{E_{11}} = -\frac{\nu_{21}}{E_{22}}$$

taking as values typical of a carbon/epoxy composite,  $E_{11} = 140$  GPa,  $E_{22} = 12$  GPa,  $G_{12} = 6$  GPa,  $\nu_{12} = 0.25$ , and  $\nu_{21} = 0.0213$ , then  $E' \approx 0.4E_{11}$ . If, alternatively, the crack is considered to lie parallel to the fibers (Fig. 2.18b), then  $E' \approx 2E_{22}$  where  $E'$  substitutes for the  $a$  terms in equation (2.35).

As long as crack propagation occurs on a plane of symmetry, the relationship between  $K_1$ ,  $\sigma$ , and  $a$  for the linear orthotropic material remains the same as that for the isotropic material. Thus, referring back to the unidirectional composite, for a given crack length  $a$  and normal stress  $\sigma$ , a crack parallel to the fibers produces a larger  $G$  than one normal to the fibers. This results from the lower compliance of the composite when stressed in the fiber direction.

In the fiber composite material, the orientation dependence of  $R$  must also be taken into consideration. In general, a composite is notch-sensitive to cracks running parallel to the fibers (Fig. 2.18b) and the fracture mechanics principles described above may be directly employed. However, the composite may not be notch-sensitive in the situation shown in Figure 2.18a. In some cases,<sup>7</sup> the composite may become notch-sensitive when  $a \gg \delta$ , the ineffective length, because the strain concentration in the matrix may then lead to fiber fractures at the crack tip. The crack would then become more effective with increasing  $a$ , as required in fracture mechanics considerations. However, in other cases, gross failure of the fiber/matrix interface may occur, resulting in the splitting mode of failure illustrated in Figure 2.18c. This situation, which occurs in more weakly bonded composites, results in complete notch-insensitivity (failure at the net section strength). Both of these situations are illustrated in some experimental work on carbon/epoxy composites in Figure 2.20, taken from Ref. 11.

The conditions for crack turning or splitting can be approached from energy considerations.<sup>15</sup> For the cracking illustrated in Figure 2.18c to occur in a unidirectional composite, it is necessary that:

$$\frac{G_1}{G_2} < \frac{R_1}{R_2} \quad (2.36)$$

where  $G_1$  is the energy release rate for self-similar propagation and  $G_2$  the release rate for splitting. Typically, for carbon/epoxy  $R_1/R_2$  is in the range 25–50 and  $G_1/G_2$  is about 20, so splitting is generally predicted.

As mentioned earlier, most advanced composite structures are made of laminates in the form of unidirectional plies laminated together at various orientations. The fracture behavior of these materials is considered in Chapter 6 and 8. In laminates, toughness is highly dependent on the degree of ply splitting and inter-ply disbonding (delamination), resulting in high-energy absorption and crack deflection.

An approach similar to that just described can be taken for this highly complex situation.<sup>16</sup> The direction of crack growth is based on the  $R_1/R_2$  ratio for each ply and the  $G_1/G_2$  ratio for the laminate. The energy release rates are calculated by finite element procedures and recalculated after each increment of crack growth until the point of catastrophic failure.

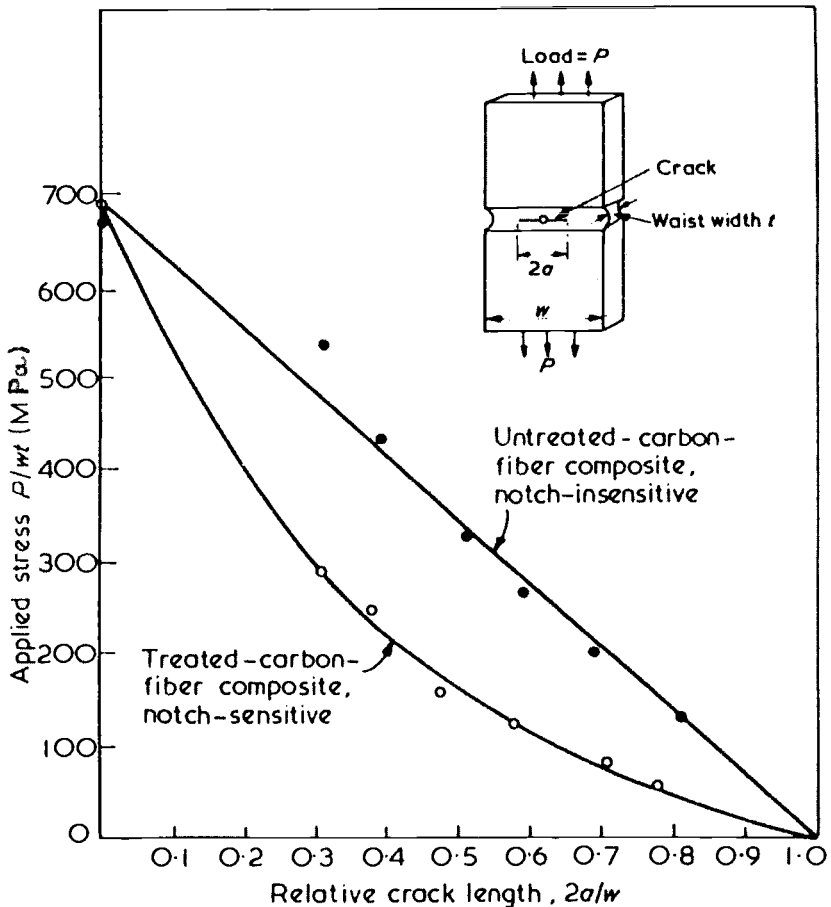


Fig. 2.20 Nominal applied stress versus relative crack size for a carbon-fiber/epoxy-composite showing notch-sensitive and notch-insensitive behavior. Taken from Ref. 11.

## References

- <sup>1</sup>Jones, R. M., *Mechanics of Composite Materials*, Scripta Book, Washington, DC, 1975.
- <sup>2</sup>Hyer, M. W., and Waas, A. M., "Micromechanics of Composite Materials," *Comprehensive Composite Materials*, edited by A. Kelly and C. Zwebin, Vol. 1, Elsevier Science Ltd, 2000.
- <sup>3</sup>Ekvall, J. C. "Structural Behaviour of Monofilament Composites" AIAA 6th Structures and Materials Conference, April 1965.
- <sup>4</sup>Fung, Y. C., *Foundations of Solid Mechanics 1965*, Prentice-Hall, Englewood Cliffs, NJ, 1965.

<sup>5</sup>Tsai, S. W., and Halpin, H. T., *Introduction to Composite Materials*, Technomic Publishing, Lancaster, PA, 1980.

<sup>6</sup>Kelly, A., and Davis, G. J., "The Principles of the Fibre Reinforcement of Metals," *Metallurgical Reviews*, Vol. 10, 1965, p. 1.

<sup>7</sup>Kelly, A., *Strong Solids*, 3rd ed., Clarendon Press, Oxford, UK, 1986.

<sup>8</sup>Daniels, H. E., "The Statistical Theory of the Strength of Bundles of Threads," *Proceedings of the Royal Society of London*, Vol. A183, 1945, p. 405.

<sup>9</sup>Rosen, B. W., "Tensile Failure of Fibrous Composites," *AIAA Journal*, Vol. 2 1964, pp. 1985–1991.

<sup>10</sup>Dow, N. F., Rosen, B.W., "Evaluations of Filament-Reinforced Composites for Aerospace Applications," NASA CR-207, April 1965.

<sup>11</sup>Philips, D. C., and Tetleman, A. S., "The Fracture Toughness of Fibre Composites," *Composites*, Vol. 3, 1972, pp. 216–223.

<sup>12</sup>Argon, A. S., "Fracture Strength and Toughness Mechanisms," Cambridge, MA, *Comprehensive Composite Materials*, edited by A. Kelly and C. Zwebin, Vol. 1, Elsevier Science, 2000.

<sup>13</sup>Lawn, B. R., and Wilshaw, T. R., *Fracture of Brittle Solids*, Cambridge University Press, Cambridge, England, UK, 1975.

<sup>14</sup>Sih, G., Paris, P. C., and Irwin, G. R., "On Cracks in Rectilinearly Anisotropic Bodies," *International Journal of Fracture Mechanics*, Vol. 1, 1965, p. 189.

<sup>15</sup>Harrison, N. L., "Splitting of Fibre-Reinforced Materials," *Fibre Science and Technology*, Vol. 6, 1973, p. 25.

<sup>16</sup>Griffith, W. I., Kanninen, M. F., and Rybicki, E. F., *A Fracture Mechanics Approach to the Analysis of Carbon/Epoxy Laminated Precracked Tension Panels*, ASTM STP 1979, p. 696.